










# Assessment of cytotoxic impact of wild grown *Lavandula angustifolia* essential oil encapsulated in liposomes and nanoemulsions on DU145 cancer cell line

Mimoza BASHOLLI-SALIHU <sup>1,2</sup> , Aida LOSHAJ-SHALA <sup>1</sup> , Art ÇUNAKU <sup>1</sup> , Venesa LUPÇI <sup>3</sup> ,  
Ufuk BAĞCI <sup>4</sup> , Entela HALOCI <sup>5</sup> , Gjoshë STEFKOV <sup>6</sup> , Toskë KRYEZIU <sup>1,2,4</sup> \* , Andreas  
ZIMMER <sup>2</sup> 

<sup>1</sup> Department of Drug Analysis and Pharmaceutical Technology, Faculty of Medicine, University of Prishtina, Prishtina, Kosovo.

<sup>2</sup> Department of Pharmaceutical Technology, Institute of Pharmaceutical Sciences, University of Graz, Graz, Austria.

<sup>3</sup> Department of General Medicine, Faculty of Medicine, University of Prishtina, Prishtina, Kosovo.

<sup>4</sup> Technology Research Development Application and Research Centre, Trakya University, Edirne, Türkiye.

<sup>5</sup> Department of Pharmacy, Faculty of Medicine, University of Medicine Tirana, Tirana, Albania.

<sup>6</sup> Institute of Pharmacognosy, Faculty of Pharmacy, Ss. Cyril and Methodius University, Skopje, North Macedonia.

\* Corresponding Author. E-mail: toske.kryeziu@uni-pr.edu (T.K.); Tel. +383-44-223 507.

Received: 9 September 2024 / Revised: 30 November 2024 / Accepted: 2 December 2024

**ABSTRACT:** The cytotoxic activity of free and nanoencapsulated essential oil of *Lavandula angustifolia* (LEO) was evaluated in this study. The aim was to produce different nanoformulations (NF) of LEO to improve the physicochemical properties of NF and the cytotoxic activity of LEO in the DU145 cancer cell line. Essential oil-based liposomes (LEO-Lipoid S100, -Ph 85G, and -Ph 90H) and nanoemulsions (LEO-NE) were prepared by ethanol injection method and high-pressure homogenization, respectively. LEO demonstrates measurable *in vitro* cytotoxic activity against the DU145 cell line (IC<sub>50</sub> 75 µg/mL). NE and Ph90H LS significantly enhanced its cytotoxic activity, while LEO-Lipoid S100 LS and LEO-Ph 85G LS showed no significant difference. LEO-Ph 90H LS and LEO-NE demonstrate stable nanosystems and enhanced cytotoxic potential against the DU-145 cancer cell line, suggesting promising therapeutic benefits for future application. Further studies involving *in vivo* experiments are necessary to validate and extend these findings.

**KEYWORDS:** *Lavandula angustifolia*; essential oil; liposome; nanoemulsion; DU145; cancer cell line.

## 1. INTRODUCTION

*Lavandula angustifolia*, often called English lavender, is the prime species within the *Lavandula* genus of the *Lamiaceae* family, which comprises over 20 distinct species. These species are widely used in the pharmaceutical, cosmetic, and agricultural sectors. Specifically, the *L. angustifolia* plant species present a diverse composition, featuring terpenes (both monoterpenes and sesquiterpenes), phenolic acids, anthocyanins, and flavonoids, all contributing to its remarkable antioxidant, cytotoxic, and antimicrobial properties. Moreover, the essential oils (EOs) derived from these plants show a broad spectrum of biological effects, including sedative, anticonvulsant, cytotoxic, anesthetic, antibacterial, carminative, and anti-bloating properties, as highlighted in studies by the literature [1,2].

The biological activity of EOs is directly related to their phytochemical composition, which is influenced by several factors, including phytochemical diversity, climatic conditions, cultivation methods (wild versus cultivated), and geographical positioning. However, the practical application of EOs in medicine and pharmaceuticals is challenged by their inherent limitations, such as high volatility, sensitivity to light and oxygen, water insolubility, and low bioavailability. These constraints significantly restrict their broader utilization in therapeutic domains [2–4].

To overcome these challenges, encapsulating EOs within nanodelivery systems has emerged as a promising strategy to address these limitations, simultaneously enhancing their physicochemical properties,

**How to cite this article:** Basholli-Saliu M, Loshaj-Shala A, Çunaku A, Lupçi V, Bağci U, Haloci E, Stefkov G, Kryeziu T, Zimmer A. Assessment of cytotoxic impact of wild grown *Lavandula angustifolia* essential oil encapsulated in liposomes and nanoemulsions on DU145 cancer cell line. J Res Pharm. 2025; 29(1): 476-485.

bioavailability, stability, and biological activity. The technique of nanoencapsulation, utilizing nanodelivery systems such as liposomes (LS) and nanoemulsions (NE), provides a viable approach to overcome the inherent deficiencies of EOs while also boosting their biological activity and stability, as evidenced by the literature [3,5].

Utilizing LS and NE to encapsulate bioactive compounds, such as EOs, offers a significant advantage, enabling improved delivery and efficacy.

Liposomes and nanoemulsions are two key nanosystems used in drug delivery, recognized for their ability to encapsulate hydrophobic and hydrophilic substances. Liposomes excel in interacting with cell membranes, while nanoemulsions enhance the solubility of lipophilic drugs without requiring organic solvents, making them safer and versatile for various applications, including the food industry. Both systems are non-toxic, biodegradable, and easy to prepare, offering effective delivery of anticancer agents and improved control over drug release profiles, which enhances stability and solubility [6–8].

The advancement of LS and NE for medical applications relied on developing methodologies capable of yielding homogeneous formulations of minimal size and showing high encapsulation efficiency. Achieving this is possible through specific preparation methods: the ethanol injection method for LS and the high-pressure homogenization method for NE. These methods are crucial in ensuring the nanosystem's desired physicochemical properties and efficacy for therapeutic purposes [9,10].

Additionally, the development of resistance by specific cancer cells to diverse therapeutic agents has increased the complexity of treatment. Therefore, integrating complementary therapies is recommended to naturally enhance the immune response while reducing the adverse effects associated with conventional treatments. Consequently, an increasing interest is in investigating the potential of encapsulating EOs in LS and NE formats as novel anticancer nanocarrier strategies [11,12].

This study aimed to develop and characterize different LS and NE that could be used to encapsulate LEO to preserve and enhance its biological activities while improving the physicochemical properties as a promising, successful therapeutic approach. In particular, the effect and comparison of three different LS nanocarriers (LEO-Lipoid S100 LS, LEO-Ph 85G LS, and LEO-Ph 90H LS) and NE (LEO-NE) on the cytotoxic activity of LEO in DU145 cancer cell line was investigated. Moreover, the stability of these nanosystems was evaluated after storage at 25°C for 1, 3, and 6 months.

## 2. RESULTS AND DISCUSSION

### 2.1. Essential Oil Composition

The analysis of Table 1 and Figure 1, employing GC/FID/MS, reveals that the predominant constituents in LEO include linalool (21.40%), linalyl acetate (17.40%), camphor (16.10%), 1,8-cineole (11.10%), and borneol (4.15%). This specific blend of components aligns with other research findings, highlighting linalool and linalyl acetate as consistently major elements in LEO from diverse geographical regions. The literature data confirms that linalool and linalyl acetate stand out as primary constituents in various species within the lavender genus (*L. angustifolia*, *L. vera*, *L. hybrida* Rev., and *L. latifolia*), even though presented at different concentrations (linalool in range of 10.0–57.5% and linalyl acetate in range of 4–55%). Conversely, in Brazilian *L. angustifolia* EO, borneol emerges as the principal component [2]. This confirms that the composition of EOs is influenced by various factors such as the plant's growth conditions, geographical origins, climate, genetic variances, extraction techniques, and the plant parts used [4]. These factors play a crucial role in defining the EO's biological characteristics. Thus, it is imperative to recognize that each EO chemical composition and biological effectiveness are distinct, necessitating individual assessment [2,13–15].

### 2.2. Characterization of liposomes and nanoemulsions

Particle/droplet size, Polydispersity Index (PDI), and Zeta Potential (ZP) were evaluated for both blank and LEO-loaded nanosystems, and the results are presented in Table 2.

**Table 1.** Chemical composition of *L. angustifolia* essential oil as determined by GC/FID/MS.

Peak No.	Compound	RT <sup>a</sup> (min)	RI <sup>b</sup>	%
1	<i>α</i> -Pinene	8.078	939	0.35
2	Camphene	8.644	953	0.36
3	<i>β</i> -Pinene	9.583	980	0.31
4	Myrcene	9.869	988	1.57

5	<i>p</i> -Cymene	11.277	1020	0.33
6	Limonene	11.471	1024	0.47
7	1,8-Cineole	11.677	1033	11.13
8	$\beta$ - <i>trans</i> -Ocimene	12.060	1040	0.86
9	Linalool oxide cis	13.131	1067	3.08
10	Linalool	14.538	1098	21.38
11	Thujone-cis	11.778	1101	0.18
12	<i>neo</i> -allo-Ocimene	15.511	1142	0.14
13	Camphor	16.638	1143	16.07
14	Lavandulol	17.084	1165	0.99
15	Borneol	17.611	1165	4.15
16	Terpinen-4-ol	17.897	1177	0.68
17	$\alpha$ -Terpineol	18.526	1189	1.32
18	Verbenone	19.036	1204	0.15
19	Nerol	19.711	1228	0.1
20	Carvone	20.603	1243	0.12
21	Linalyl acetate	20.941	1256	17.39
22	Lavandulyl acetate	22.263	1288	2.51
23	Neryl acetate	25.456	1365	0.58
24	Geranyl acetate	26.314	1383	1.19
25	Sesquithujene-7-epi	26.755	1390	0.2
26	Sesquithujene	27.367	1405	0.15
27	$\alpha$ -Bergamoten-cis	27.865	1411	0.19
28	<i>trans</i> (E) -Caryophyllene	28.191	1418	2.87
29	$\beta$ -Duprezianene	29.123	1421	0.15
30	Z- $\beta$ -Farnesene	29.421	1440	0.39
31	$\alpha$ -Humulene	29.638	1452	0.31
32	Ar-Curcumene	30.634	1479	0.13
33	Lavandulyl isovalerate	31.418	1509	0.58
34	g-Cadinene	31.944	1513	0.3
35	Caryophyllene oxide	34.702	1581	0.83
36	$\alpha$ -Cadinol-epi	36.934	1638	0.14
37	Triacontane	64.045	3000	0.66
<b>Total:</b>				<b>92.31</b>

<sup>a</sup> RT (min) = Retention time<sup>b</sup> RI = Retention index<sup>c</sup> The percentages of compounds were obtained by FID peak-area normalization. The percentage composition of the oil was computed by the normalization method from the GC peak areas, calculated as the mean of three samples without correction factors.

Significant size variations were observed among the blank LS prepared with different phospholipids ( $p < 0.001$ ). Blank LS with Lipoid S100 had a larger particle size ( $270 \pm 1.50$  nm) compared to Ph 90H LS ( $161 \pm 3.60$  nm) and Ph 85G LS ( $81 \pm 1.90$  nm) ( $p < 0.001$ ). The blank NE had a smaller droplet size ( $114 \pm 1.72$  nm). Incorporating LEO increased the size of Lipoid S100 LS to  $138 \pm 2.75$  nm ( $p < 0.001$ ), while Ph 85G LS size remained similar at  $87 \pm 2.97$  nm ( $p > 0.05$ ). LEO-NE showed a size of  $96 \pm 0.71$  nm ( $p < 0.001$ ). These size changes could be due to LEO's impact on the nanosystem membranes, potentially reducing cohesive forces among components [5,16].

The Polydispersity Index (PDI) data indicated that blank NE had the highest uniformity ( $0.19 \pm 0.01$ ), followed by blank Lipoid S100 LS ( $0.22 \pm 0.05$ ) and Ph 85G LS ( $0.30 \pm 0.01$ ). Ph 90H LS had less uniformity ( $0.38 \pm 0.03$ ), significantly different from blank Lipoid S100 LS ( $p < 0.01$ ) but not from blank Ph 85G LS ( $p > 0.05$ ). LEO-loaded Lipoid S100 LS had a PDI of  $0.09 \pm 0.01$  ( $p < 0.05$ ), while LEO-Ph 85G LS and Ph 90H LS PDIs were similar to their blanks. LEO-NE showed improved PDI at  $0.11 \pm 0.01$  ( $p < 0.001$ ). A PDI of 0.30 or below indicates satisfactory uniformity, ensuring consistent pharmacokinetics and distribution [17,18].

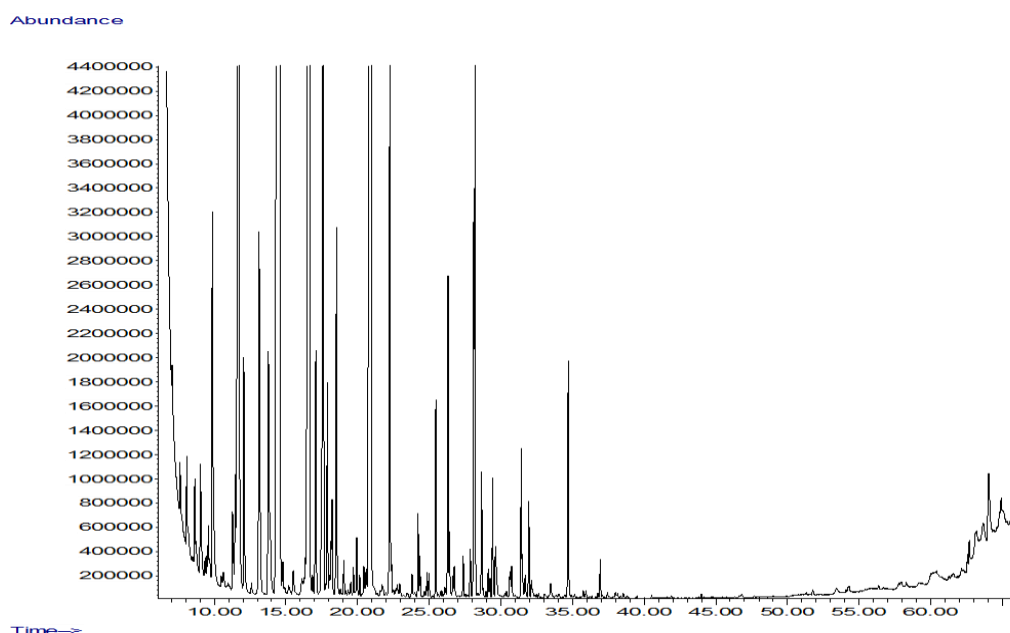


**Figure 1.** GC/FID/MS chromatogram of *L. angustifolia* essential oil.

**Table 2** Characteristics of blank and *L. angustifolia* essential oil loaded liposomes and nanoemulsions regarding mean particle/ droplet size, polydispersity index (PDI), zeta potential (ZP), and encapsulation efficiency (EE%).

Nanoformulation batches		Mean size (nm)	PDI <sup>c</sup>	ZP <sup>d</sup> (mV)	EE% <sup>e</sup>
<b>Lipoid S100 LS<sup>a</sup></b>	Empty LS	270 ± 1.50	0.22 ± 0.05	- 4.20 ± 0.70	
	LEO-LS	138 ± 2.75	0.09 ± 0.01	- 9.10 ± 0.55	68.28 ± 4.43
<b>Ph 85G LS</b>	Empty LS	81 ± 1.90	0.30 ± 0.01	- 35.40 ± 0.90	
	LEO-LS	87 ± 2.97	0.25 ± 0.01	- 35.70 ± 0.64	66.32 ± 2.50
<b>Ph 90H LS</b>	Empty LS	161 ± 3.60	0.38 ± 0.03	- 11.60 ± 0.10	
	LEO-LS	159 ± 3.38	0.35 ± 0.08	- 12.90 ± 0.15	69.41 ± 1.31
<b>NE<sup>b</sup></b>	Empty NE	114 ± 1.72	0.19 ± 0.01	- 7.51 ± 0.50	
	LEO-NE	96 ± 0.71	0.11 ± 0.01	- 32.13 ± 1.36	75.43 ± 0.89

<sup>a</sup> LS: liposome; <sup>b</sup> NE: nanoemulsion; <sup>c</sup> PDI: polydispersity index; <sup>d</sup> ZP: zeta potential.

<sup>e</sup> EE%: encapsulation efficiency.

Data are expressed as a mean value ± standard deviation (n = 3).

The literature reveals that LS containing LEO exhibited low ZP values: -3.73 mV. This crucial stability indicator suggests values around -30 mV were mainly observed in all Ph 85G LS and NE after LEO encapsulation. ZP measurements showed blank Ph 85G LS had favorable results (-35.40 ± 0.90 mV), followed by Ph 90H LS (-11.60 ± 0.10 mV), blank NE (-7.51 ± 0.50 mV), and Lipoid S100 LS (-4.20 ± 0.70 mV). LEO encapsulation did not significantly alter ZP for Ph 85G- and Ph 90H-LS. However, Lipoid S100 LS showed a lower ZP of -9.10 ± 0.55 mV after LEO encapsulation, and LEO-NE had a significant change to -32.13 ± 1.36 mV ( $p < 0.001$ ). Negative ZP values suggest colloidal stability, which is crucial for preventing aggregation and extending circulation time [19–21].

This study's results show that NE and LS achieved high EE%, as illustrated in Table 2. Specifically, LEO-Lipoid S100 LS achieved an EE% of 68.28% ± 4.43, while LEO-Ph 85G LS had an EE% of 66.32% ± 2.50, and LEO-Ph 90H LS reached an EE% of 69.41% ± 1.31, with no significant differences among them ( $p > 0.05$ ). NE exhibited an EE% of 75.43 ± 0.89. These findings align with previous literature, indicating that when EOs are encapsulated sufficiently within nanosystems, the EE% typically approaches a value of around 60%,

depending on the type of EO used. This observation aligns with and extends the current literature, suggesting that the EE% may be influenced by the nanosystems composition and the specific type of EO incorporated, as suggested by previous studies [18,22,23].

### 2.3. Cytotoxic potential

The cytotoxic effects of LEO and its nanosystems were assessed *in vitro* on the DU145 cancer cell line, and the results are presented in Figure 2. This study found that LEO had measurable *in vitro* cytotoxic activity against the DU145 prostate cancer cell line. The IC<sub>50</sub> of LEO was determined to be 75 µg/mL. Our results align with previous studies that reported the cytotoxicity of LEO against various cell lines, indicating that LEO from different countries exhibited different cytotoxic activities – EO from *L. angustifolia* exhibits, in some cases, unsatisfactory cytotoxic effects [1,2]. The literature reported that linalyl acetate demonstrated a more potent cytotoxic effect than LEO. This indicates that other factors in the EO may be inhibiting its cytotoxic activity. Furthermore, LEO (originating from Palestine), with the main components linalool and linalyl acetate, exhibited potent cytotoxic effects on DU145 and PC-3 cells [24].

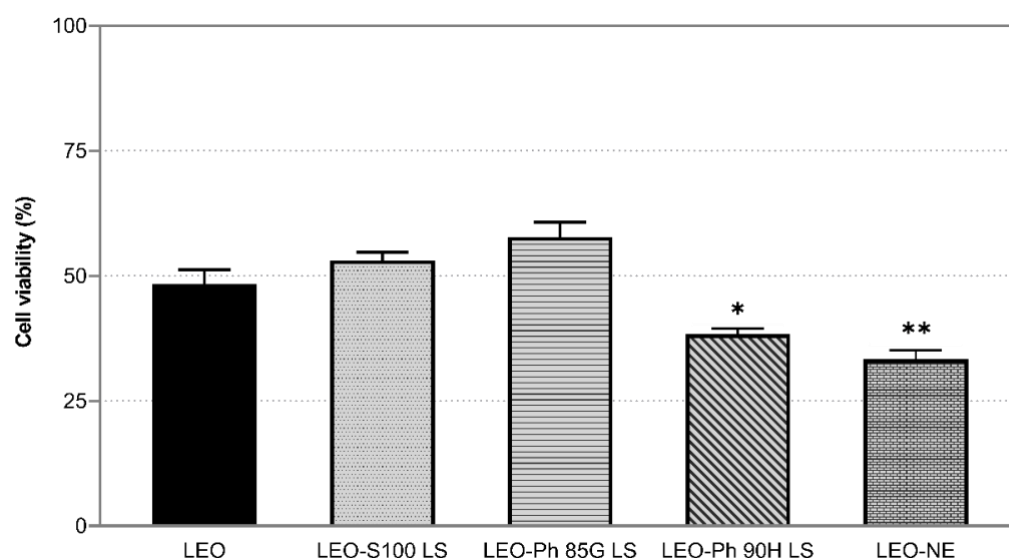


**Figure 2.** Cytotoxicity of free *L. angustifolia* essential oil (LEO) and nanoencapsulated LEO on DU145 cancer cell line. The chart shows cell viability post-treatment with free essential oil and essential oil encapsulated in Lipoid S100 liposomes, Phospholipon 85G liposomes, Phospholipon 90H liposomes, and nanoemulsion, as assessed by the MTT method.

\*\* indicates a statistically significant value of  $p < 0.01$

\* indicates a statistically significant value of  $p < 0.05$

Each bar represents  $\pm$  SD ( $n = 3$ ).

It is indicated that the cytotoxic action of EOs is not solely dependent on the components with the highest concentrations, suggesting an interaction among the phytochemical components of EOs at various concentrations. Consequently, even components present in trace amounts could play a role in the overall cytotoxic effect of EOs. Therefore, the cytotoxic effect of each EO from the same genus cannot be generalized and should be determined individually [25–27].

The integration of LEO into LS and NE modified the viability of the cancer cell line examined in this research. The findings indicated that LEO-NE demonstrated enhanced cytotoxic activity *in vitro* compared to the free LEO. As far as we know, the cytotoxic impacts of different LEO LS and NE nanosystems on the DU145 cancer cell line have not been previously explored.

The encapsulation of LEO into NE markedly enhanced its cytotoxic activity, decreasing the cell viability of DU145 cancer cells to  $33.34\% \pm 2.55$  ( $p < 0.01$ ). This increase in cytotoxic activity post-encapsulation in NE aligns with findings documented in earlier research [7]. As illustrated in Figure 2, LEO-Ph90H LS exhibited significantly higher cytotoxicity than the unencapsulated LEO ( $p < 0.05$ ), with reduced cell viability to  $38.72\% \pm 1.98$ . Conversely, the cytotoxic effects of LEO-Lipoid S100 LS and LEO-Ph 85G LS were not significantly different from those of the free LEO ( $p > 0.05$ ), with cell viability  $53.07\% \pm 2.87$  and  $57.78\% \pm 5.10$ , respectively ( $p > 0.05$ ). The control formulations without active ingredients displayed no cytotoxic activity.



The enhanced cytotoxic activity of LEO-NE and LEO 90H can be attributed to their increased ability to be trapped inside cells compared to non-encapsulated LEO. Studies have shown that encapsulation in NE enhances intracellular accumulation and stability of LEO, leading to sustained release and improved cytotoxicity. LEO-NE significantly improved cytotoxic activity ( $p < 0.001$ ) without affecting the viability of normal cell lines, highlighting the suitability of EOs as anticancer agents. Additionally, nanodelivery systems increase intracellular uptake and accumulation, enhancing cytotoxic activity compared to free EO. Furthermore, the differences observed among the three LS formulations and NE may be attributed to LS's physical and chemical instability containing unsaturated components, which can reduce efficacy [28–30].

## 2.4. Stability Studies

Variables such as particle size, ZP, and storage conditions influence the stability of LS and NE [18,22]. This study examined the particle size, PDI, and ZP of LEO-encapsulated nanosystems before and after 1, 3, and 6 months of storage at 25 °C (Table 3). LEO-NE showed a significant change in droplet size at  $172 \pm 18.17$  nm ( $p < 0.001$ ), with a PDI of  $0.61 \pm 0.03$  ( $p < 0.001$ ) and a ZP of  $-28.16 \pm 0.16$  mV ( $p < 0.05$ ). The viscosity increased significantly at  $1.66 \pm 0.07$  mPa.s ( $p < 0.001$ ).

**Table 3.** Characteristics of blank and *L. angustifolia* essential oil-loaded liposomes and nanoemulsions in terms of mean droplet size, PDI, and zeta potential.

	Time interval	Mean size (nm)	PDI <sup>c</sup>	ZP <sup>d</sup> (mV)
<b>Lipoid S100 LS<sup>a</sup></b>	Day 1	$138 \pm 2.75$	$0.09 \pm 0.01$	$-9.10 \pm 0.55$
	After 1 month	$168 \pm 3.80$	$0.23 \pm 0.02$	$-20.55 \pm 1.08$
	After 3 months	$288 \pm 3.60$	$0.40 \pm 0.04$	$-14.8 \pm 0.62$
	After 6 months	$1687 \pm 19.80$	$0.49 \pm 0.06$	$-8.50 \pm 0.41$
<b>Ph 85G LS</b>	Day 1	$87 \pm 2.97$	$0.25 \pm 0.01$	$-35.70 \pm 0.64$
	After 1 month	$125 \pm 2.77$	$0.44 \pm 0.06$	$-38.70 \pm 2.03$
	After 3 months	$297 \pm 4.20$	$0.53 \pm 0.02$	$-15.3 \pm 0.22$
	After 6 months	$5479 \pm 28.28$	$0.71 \pm 0.04$	$-13.00 \pm 0.42$
<b>Ph 90H LS</b>	Day 1	$159 \pm 3.38$	$0.35 \pm 0.08$	$-12.90 \pm 0.15$
	After 1 month	$121 \pm 0.72$	$0.30 \pm 0.01$	$-10.50 \pm 0.05$
	After 3 months	$142 \pm 2.59$	$0.33 \pm 0.01$	$-21.5 \pm 0.15$
	After 6 months	$164 \pm 22.16$	$0.68 \pm 0.05$	$-20.64 \pm 0.62$
<b>NE<sup>b</sup></b>	Day 1	$96 \pm 0.71$	$0.11 \pm 0.01$	$-32.13 \pm 1.36$
	After 1 month	$89 \pm 0.545$	$0.21 \pm 0.01$	$-26.30 \pm 2.21$
	After 3 months	$93 \pm 0.22$	$0.43 \pm 0.02$	$-28.40 \pm 0.55$
	After 6 months	$172 \pm 18.17$	$0.61 \pm 0.03$	$-28.16 \pm 0.16$

<sup>a</sup> LS: liposome; <sup>b</sup> NE: nanoemulsion; <sup>c</sup> PDI: polydispersity index; <sup>d</sup> ZP: zeta potential.

Data are expressed as a mean value  $\pm$  standard deviation ( $n = 3$ ).

The study found that LEO-Ph 90H LS remained stable over six months, averaging  $164 \pm 22.16$  nm ( $p > 0.05$ ). The PDI and ZP were significantly adjusted to  $0.68 \pm 0.05$  and  $-20.64 \pm 0.62$  mV ( $p < 0.001$ ), respectively, but remained within acceptable ranges for stability. After six months of storage, LEO-Lipoid S100 LS and LEO-Ph 85G LS demonstrated fewer stable results. The particle size of LEO-Lipoid S100 LS and LEO-Ph 85G LS increased significantly to  $1687 \pm 19.80$  nm and  $5479 \pm 28.28$  nm ( $p < 0.001$ ), respectively. PDI values increased to  $0.49 \pm 0.06$  and  $0.71 \pm 0.04$  ( $p < 0.001$ ), respectively, while ZP values were  $-8.50 \pm 0.41$  mV and  $-13.00 \pm 0.42$  mV ( $p < 0.001$ ). The viscosity was found to be  $1.43 \pm 0.71$  mPa.s ( $p > 0.05$ ) and  $2.31 \pm 0.18$  mPa.s ( $p < 0.001$ ). These results show that these two LSs were unstable for six months of storage.

The stability of LS and NE is attributed to the composition of the nanoformulation, which includes the ratio of the respective LS components, size, and ZP. Larger particles tend to aggregate because they are more susceptible to the influence of Brownian motion, giving them more chances to collide. ZP is also essential for LS's stability and aggregation behavior. This could explain previous data indicating that nanosystems with smaller vesicles are sometimes less stable [31].

Regarding NE, they remained stable after six months of storage with no significant differences in size:  $172 \pm 18.17$  nm, PDI:  $0.61 \pm 0.03$ , and ZP:  $-28.16 \pm 0.16$  mV ( $p > 0.05$ ).

### 3. CONCLUSION

Our investigation marks a pioneering step in exploring the LS and NE's cytotoxic of LS and NE encapsulating LEO, particularly on wild species. This study is the first to evaluate and compare the effects of LEO on different nanosystems, highlighting the enhanced cytotoxic activity of LEO-NE and LEO-Ph 90H LS against prostate cancer cell lines. The encapsulation of LEO within Ph 85G LS and Lipoid S100 LS was able to maintain cytotoxic properties compared to their unencapsulated counterparts. These findings underscore the significance of stable LS and NE in improving the effectiveness of LEO as a potential future anticancer agent.

By demonstrating LEO's cytotoxic potential against prostate cancer cells and the benefits of its nanosystem encapsulation, our research contributes valuable insights to the ongoing quest for effective cancer therapy candidates. The promising outcomes suggest that LEO, mainly when delivered through NE and LS, merits further investigation and development as a potential candidate for cancer treatment. This endeavor could pave the way for innovative, more effective therapeutic strategies against cancer, harnessing the power of nanotechnology and natural compounds.

### 4. MATERIALS AND METHODS

#### 4.1. Chemicals

MTT (thiazolyl blue tetrazolium bromide), hexane, 95% cholesterol, and absolute ethanol (HPLC grade) were obtained from Sigma-Aldrich (Germany). Additionally, DMSO (Dimethyl sulfoxide), Trypsin-EDTA, and cell nutrient medium composed of Dulbecco's Minimum Essential Medium (DMEM) and HAM'S F12 in a 1:1 ratio were sourced from Sigma-Aldrich (Germany). Lipoid S100, Phospholipon 85G, and Phospholipon 90H were acquired from Lipoid (Germany). Polysorbate (Tween 80) and Lecithin were sourced from Caelo and ROTH (Germany). Medium Chain Triglycerides (MCT) were purchased from Herba Chemosan Apotheke (Austria). The dialysis membranes ZelluTrans/ROTH T1 (MWCO: 3500) were supplied by Zellu Carl Roth (Austria). The human cell line (DU145) was obtained from the American Type Culture Collection (ATCC).

#### 4.2. Plant material and essential oil extraction

Aerial parts of *L. angustifolia* were collected from Albania's northern region for EO extraction. Professor Skerdilaid Xhulaj identified the specimens, and voucher specimens were deposited at the University of Tirana Herbarium. The plant materials were air-dried at room temperature before hydrodistillation using a Clevenger-type apparatus. The EO was then dried using anhydrous sodium sulfate and stored at four °C, following the methodology detailed in the literature [18,32].

#### 4.3. Essential oil analysis by GC/FID/MS

The composition of the LEO was determined using an Agilent 7890A Gas Chromatography system equipped with an FID detector and an Agilent 5975C Mass Quadrupole detector. The setup used an HP-5 ms capillary column (30 m × 0.25 mm, film thickness 0.25 µm) with specific conditions: Starting at 60 °C (0 min). The oven temperature was gradually increased at a rate of 3 °C/min and then to 280 °C at a rate of 10 °C/min for another minute; helium served as the carrier gas at a flow rate of 1 mL/min; the injector and FID detector temperatures were kept at 220 °C and 270 °C, respectively, with a 1:1 split ratio for sample injection. For mass spectrometry, settings included an ionization voltage of 70 eV, an ion source temperature of 230 °C, a transfer line temperature of 280 °C, and a mass range of 50–550 Da, with the spectrometer set to scan mode. Compound identification was accomplished by comparing mass spectra to those in the Adams, NIST, and Wiley databases, as well as literature mass spectra, using homologous series of normal alkanes (C9–C25) under AMDIS conditions and Kovat's indices from literature [33]. The normalization method was used to quantify GC-FID peak areas, with no correction factors applied.

#### 4.4. Liposome preparation

The ethanol injection method was used to prepare both blank and LEO-loaded LS, as described in the literature [5,18]. This entailed dissolving phospholipids (either Lipoid S100, Phospholipon 85G, or Phospholipon 90H) at a concentration of 10 mg/mL, LEO at 2.5 mg/mL, and cholesterol at 5 mg/mL in 10 mL of absolute ethanol. The solution was mixed with a magnetic stirrer. The organic phase was then slowly injected into 20 mL of Milli-Q water at a 1 mL/min rate with a syringe pump. This process led to the spontaneous formation of LS. After injection, the LS were stirred for 15 minutes to ensure uniformity.

Ethanol was removed through dialysis using ZelluTrans/ROTH T1 membranes for 16 hours, stirring continuously in 1000 mL of dialysis medium. Batches without LEO served as blank LS. Each LS batch was prepared three times. Before any further analysis, all LS batches were kept at four °C.

#### 4.5. Nanoemulsion preparation

An optimized NE formulation method was developed with Prof. Dr. Andreas Zimmer's team at the University of Graz, Austria. This method required separate preparation steps for the oil and water phases. The oil phase combined 1.5 g of lecithin with 8.5 g of MCT for a total of 10 g. Simultaneously, the water phase involved dissolving 1.5 g of Polysorbate 80 dissolved in distilled water, yielding 150 g of solution. Both phases were heated to 75 °C and homogenized separately. The NE formulation began with a pre-homogenization blend of the two phases at 8,000 rpm using an IKA T25 Ultra-Turrax for a set duration. The NE was then homogenized at 800 bar for eight cycles with a GEA Niro Soavi NS1001L2K machine. LEO was then added and stirred for two hours. The completed LEO-NEs were stored at four °C for subsequent evaluations alongside control samples of blank NEs without EOs.

#### 4.6. Particle size, PDI, and zeta potential

The study investigated the properties of LEO-loaded nanosystems, such as particle/droplet size, polydispersity index (PDI), zeta potential (ZP), and encapsulation efficiency (EE%). A Malvern Zetasizer Nano ZS (Model ZEN3500) was used to measure the mean particle/droplet size, PDI, and ZP of the blank and LEO-loaded nanosystems. After 2 minutes of equilibration time, 1 mL of the sample was inserted into the folded capillary cell (provided by Malvern), and the ZP measurements were obtained using Smoluchowski's equation. The analyses were performed thrice at a constant temperature of 25 °C, with a 2 min equilibration time. Results are reported as means  $\pm$  SD (n = 3).

#### 4.7. Determination of encapsulation efficiency

The method for determining EE% (encapsulation efficiency) was slightly adjusted from the literature [34,35]. This involved centrifuging the LS and NE suspension at 4,000 rpm for 30 minutes. Then, 2 mL of the supernatant was combined with an equal volume of hexane. The encapsulated LEO quantity was measured using a UV 1800 UV-Vis spectrophotometer at a wavelength of  $\lambda = 306$  nm. The process was repeated three times to ensure accuracy. A standard curve was created to determine LEO concentration using various concentrations of LEO dissolved in hexane. The encapsulation efficiency was calculated using the formula:

$$EE\% = \frac{(\text{Total oil} - \text{Free oil})}{\text{Total oil}} \times 100$$

#### 4.8. Determination of Cytotoxicity with an MTT Assay

The DU145 cell line, obtained from the American Type Culture Collection (ATCC®), was cultured in a 1:1 mixture of Dulbecco's Modified Eagle Medium (DMEM) and HAM's Nutrient Mixture F12 nutrient medium, which contained 10% fetal bovine serum (FBS), 100 IU/mL penicillin, 10 mg/mL streptomycin, and 1% L-glutamine. The cultures were maintained in a 5% CO<sub>2</sub> incubator. DU145 cells were seeded in 96-well plates at 7×10<sup>3</sup> cells per well (180  $\mu$ L) density and incubated for 24 hours at 37 °C in a 5% CO<sub>2</sub> atmosphere. LEO was initially solubilized in DMSO to create a 100 mg/mL stock solution, diluted with culture medium before being added to the wells. After 24 hours of incubation, 20  $\mu$ L of the LEO solution (0.39 to 200  $\mu$ g/mL) was dispensed into the wells to determine the IC<sub>50</sub>.

Separately, 20  $\mu$ L of LEO-loaded nanosystems were applied to the cells. After 24 hours of incubation, MTT solutions (20  $\mu$ L/200  $\mu$ L per well of a 5 mg/mL solution) were pipetted into each well. The plates were then incubated for another four hours at 37 °C. Subsequently, 200  $\mu$ L of DMSO was introduced to each well. The optical density of each well was measured at a wavelength of 492 nm using a microplate reader. Based on these absorbance readings, the percentage of cell viability and the IC<sub>50</sub> were calculated using the following formula:

$$\text{Cell Viability (\%)} = \frac{\text{Sample absorbance value}}{\text{Control absorbance value}} \times 100$$

In each analysis, the baseline for comparison was established by normalizing the untreated control group to 100%, with the results from treated samples being presented as a percentage relative to this control.



This cytotoxicity assay was carefully repeated three times using the protocol described in previous research. The findings were documented as mean  $\pm$  SD ( $n = 3$ ).

#### 4.9. Stability

The stability of LEO-loaded nanosystems was assessed after 1, 3, and 6 months of storage at 25 °C, including particle/droplet size, PDI, and ZP measurements. The prepared nanosystems were stored under specific conditions in a Memmert Climate Chamber ICH110, which maintained a temperature of 25 °C  $\pm$  2 °C and a relative humidity of 60%  $\pm$  5%.

#### 4.10. Statistical analysis

All analyses were carried out in triplicate and expressed as a mean value  $\pm$  SD ( $n = 3$ ). Statistical analyses were performed using GraphPad Prism 9 (GraphPad Software Inc., USA), specifically using one-way ANOVA and Tukey multiple comparison tests for all study groups. Values of  $p < 0.05$  were considered statistically significant.

**Acknowledgements:** The authors appreciate the support from the Institute of Pharmaceutical Sciences, Faculty of Natural Sciences, University of Graz (Austria), and Trakya University, Technology Research, and Development Centre (TÜTAGEM) (Edirne, Turkey) to conduct part of the experimental work.

**Author contributions:** Concept – M.B.; Design – T.K.; Supervision – A.Z., T.K.; Resources – M.B.; Materials – M.B., T.K., U.B., E.H.; Data Collection and/or Processing – M.B., A.L., T.K.; Analysis and/or Interpretation – M.B., A.L., E.H.; Literature Search – A.Ç., V.L., M.B.; Writing – M.B., T.K.; Critical Reviews – M.B., T.K., U.B., Gj.S., A.Z.

**Conflict of interest statement:** The authors declared no conflict of interest.

#### REFERENCES

- [1] Denner SS. *Lavandula angustifolia* Miller: English Lavender. *Holist Nurs Pract*. 2009; 23(1): 57-64. <https://doi.org/10.1097/01.HNP.0000343210.56710.fc>
- [2] Pérez-González C, Pérez-Ramos J, Méndez-Cuesta CA, Serrano-Vega R, Martell-Mendoza M, Pérez-Gutiérrez S. Cytotoxic activity of essential oils of some species from Lamiaceae family. In: Istifli ES, Ila HB. (Eds). *Cytotoxicity - Definition, Identification, and Cytotoxic Compounds*. IntechOpen, United Kingdom, 2019, pp. 29-43. <https://doi.org/10.5772/intechopen.86392>
- [3] da Silva LR, Ferreira OO, Cruz JN, Franco CD, Dos Anjos TO, Cascaes MM, da Costa WA, de Aguiar Andrade EH, de Oliveira MS. Lamiaceae essential oils, phytochemical profile, antioxidant, and biological activities. *Evid Based Complement Alternat Med*. 2021; 2021(1): 6748052. <https://doi.org/10.1155/2021/6748052>
- [4] Caprari C, Fantasma F, Monaco P, Divino F, Iorizzi M, Ranalli G, Fasano F, Saviano G. Chemical profiles, in vitro antioxidant and antifungal activity of four different *Lavandula angustifolia* L. EOs. *Molecules*. 2023; 28(1): 392. <https://doi.org/10.3390/molecules28010392>
- [5] Sebaaly C, Jraij A, Fessi H, Charcosset C, Greige-Gerges H. Preparation and characterization of clove essential oil-loaded liposomes. *Food Chem*. 2015; 178(2015): 52-62. <https://doi.org/10.1016/j.foodchem.2015.01.067>
- [6] Çağdaş M, Sezer AD, Bucak S. Liposomes as potential drug carrier systems for drug delivery. Application of nanotechnology in drug delivery. IntechOpen, United Kingdom, 2014, pp. 1-50. <https://doi.org/10.5772/58459>
- [7] Marchese E, D'onofrio N, Balestrieri ML, Castaldo D, Ferrari G, Donsi F. Bergamot essential oil nanoemulsions: Antimicrobial and cytotoxic activity. *Z Für Naturforschung C*. 2020; 75(7-8): 279-290. <https://doi.org/10.1515/znc-2019-0229>
- [8] Lu H, Zhang S, Wang J, Chen Q. A review on polymer and lipid-based nanocarriers and its application to nano-pharmaceutical and food-based systems. *Front Nutr*. 2021; 8(1): 783831. <https://doi.org/10.3389/fnut.2021.783831>
- [9] Nirmala MJ, Nagarajan R. Recent research trends in fabrication and applications of plant essential oil based nanoemulsions. *High Press Homog*. 2017; 8(2): 434. <https://doi.org/10.4172/2157-7439.1000434>
- [10] Gouda A, Sakr OS, Nasr M, Sammour O. Ethanol injection technique for liposomes formulation: An insight into development, influencing factors, challenges and applications. *J Drug Deliv Sci Technol*. 2021; 61(2021): 102174. <https://doi.org/10.1016/j.jddst.2020.102174>
- [11] Pontes-Quero GM, Esteban-Rubio S, Pérez Cano J, Aguilar MR, Vázquez-Lasa B. Oregano essential oil micro- and nanoencapsulation with bioactive properties for biotechnological and biomedical applications. *Front Bioeng Biotechnol*. 2021; 9(1): 703684. <https://doi.org/10.3389/fbioe.2021.703684>
- [12] AbouAitah K, Lojkowski W. Nanomedicine as an emerging technology to foster application of essential oils to fight cancer. *Pharmaceutics*. 2022; 15(7): 793. <https://doi.org/10.3390/ph15070793>
- [13] Herraiz-Peñalver D, Cases MÁ, Varela F, Navarrete P, Sánchez-Vioque R, Usano-Aleman J. Chemical characterization of *Lavandula latifolia* Medik. essential oil from Spanish wild populations. *Biochem Syst Ecol*. 2013; 46(2013): 59-68. <https://doi.org/10.1016/j.bse.2012.09.018>

- [14] Aprotosoia AC, Gille E, Trifan A, Luca VS, Miron A. Essential oils of *Lavandula* genus: a systematic review of their chemistry. *Phytochem Rev.* 2017; 16(2017): 761-799. <https://doi.org/10.1007/s11101-017-9517-1>
- [15] Niksic H, Becic F, Koric E, Gusic I, Omeragic E, Muratovic S, Miladinovic B, Duric K. Cytotoxicity screening of *Thymus vulgaris* L. essential oil in brine shrimp nauplii and cancer cell lines. *Sci Rep.* 2021; 11(1): 1-9. <https://doi.org/10.1038/s41598-021-92679-x>
- [16] Kryeziu TL, Haloci E, Loshaj-Shala A, Bagci U, Oral A, Stefkov GJ, Zimmer A, Basholli-Saliu M. Nanoencapsulation of *Origanum vulgare* essential oil into liposomes with anticancer potential. *Pharm- Int J Pharm Sci.* 2022; 77(6): 172-178. <https://doi.org/10.1691/ph.2022.1230>
- [17] Danaei MR, Dehghankhold M, Ataei S, Hasanzadeh Davarani F, Javanmard R, Dokhani A, Khorasani S, Mozafari MR. Impact of particle size and polydispersity index on the clinical applications of lipidic nanocarrier systems. *Pharmaceutics.* 2018; 10(2): 57. <https://doi.org/10.3390/pharmaceutics10020057>
- [18] Kryeziu T, Bađci U, Loshaj-Shala A, Oral A, Stefkov GJ, Zimmer A, Basholli-Saliu M. Cytotoxic activity of liposomal *Thymus capitatus* essential oil on HT-29 human colorectal cancer cell line. *Pharm- Int J Pharm Sci.* 2024; 79(3-4): 49-56. <https://doi.org/10.1691/ph.2024.3037>
- [19] Faraji Z, Shakarami J, Varshosaz J, Jafari S. Encapsulation of essential oils of *Mentha pulegium* and *Ferula gummosa* using nanoliposome technology as a safe botanical pesticide. *J Appl Biotechnol Rep.* 2020; 7(4): 237-242. <https://doi.org/10.30491/JABR.2020.121704>
- [20] Aguilar-Pérez KM, Medina DI, Narayanan J, Parra-Saldívar R, Iqbal HM. Synthesis and nano-sized characterization of bioactive oregano essential oil molecule-loaded small unilamellar nanoliposomes with antifungal potentialities. *Molecules.* 2021; 26(10): 2880. <https://doi.org/10.3390/molecules26102880>
- [21] de Alteriis E, Maione A, Falanga A, Bellavita R, Galdiero S, Albarano L, Salvatore MM, Galdiero E, Guida M. Activity of free and liposome-encapsulated essential oil from *Lavandula angustifolia* against persister-derived biofilm of *Candida auris*. *Antibiotics.* 2021; 11(1): 26. <https://doi.org/10.3390/antibiotics11010026>
- [22] Sherry M, Charcosset C, Fessi H, Greige-Gerges H. Essential oils encapsulated in liposomes: a review. *J Liposome Res.* 2013; 23(4): 268-275. <https://doi.org/10.3109/08982104.2013.819888>
- [23] Lu WC, Huang DW, Wang CC, Yeh CH, Tsai JC, Huang YT, Li PH. Preparation, characterization, and antimicrobial activity of nanoemulsions incorporating citral essential oil. *J Food Drug Anal.* 2018; 26(1): 82-89. <https://doi.org/10.1016/j.jfda.2016.12.018>
- [24] Zhao Y, Chen R, Wang Y, Qing C, Wang W, Yang Y. In vitro and in vivo efficacy studies of *Lavender angustifolia* essential oil and its active constituents on the proliferation of human prostate cancer. *Integr Cancer Ther.* 2017; 16(2): 215-226. <https://doi.org/10.1177/1534735416645408>
- [25] Elshafie HS, Camele I. An overview of the biological effects of some mediterranean essential oils on human health. *BioMed Res Int.* 2017; 2017(1): 9268468. <https://doi.org/10.1155/2017/9268468>
- [26] Leyva-López N, Gutiérrez-Grijalva EP, Vazquez-Olivo G, Heredia JB. Essential oils of oregano: Biological activity beyond their antimicrobial properties. *Molecules.* 2017; 22(6): 989. <https://doi.org/10.3390/molecules22060989>
- [27] Blažičková M, Blaško J, Kubinec R, Kozics K. Newly synthesized thymol derivative and its effect on colorectal cancer cells. *Molecules.* 2022; 27(9): 2622. <https://doi.org/10.3390/molecules27092622>
- [28] Celia C, Trapasso E, Locatelli M, Navarra M, Ventura CA, Wolfram J, Carafa M, Morittu VM, Britti D, Di Marzio L, Paolino D. Anticancer activity of liposomal bergamot essential oil (BEO) on human neuroblastoma cells. *Colloids Surf B Biointerfaces.* 2013; 112(2013): 548-553. <https://doi.org/10.1016/j.colsurfb.2013.09.017>
- [29] Abd-Rabou AA, Edris AE. Cytotoxic, apoptotic, and genetic evaluations of *Nigella sativa* essential oil nanoemulsion against human hepatocellular carcinoma cell lines. *Cancer Nanotechnol.* 2021; 12(1): 28. <https://doi.org/10.1186/s12645-021-00101-y>
- [30] Haro-González JN, Martínez-Velázquez M, Castillo-Herrera GA, Espinosa-Andrews H. Clove essential oil nanoemulsions: Development, physical characterization, and anticancer activity evaluation. *J Dispers Sci Technol.* 2024; 1-9. <https://doi.org/10.1080/01932691.2024.2302067>
- [31] Nasr G, Greige-Gerges H, Elaissari A, Khreich N. Liposome permeability to essential oil components: a focus on cholesterol content. *J Membr Biol.* 2021; 254(4): 381-395. <https://doi.org/10.1007/s00232-021-00180-3>
- [32] Papajani V, Haloci E, Goci E, Shkreli R, Manfredini S. Evaluation of antifungal activity of *Origanum vulgare* and *Rosmarinus officinalis* essential oil before and after inclusion in  $\beta$ -cyclodextrine. *Int J Pharm Pharm Sci.* 2015; 7(5): 270-273.
- [33] Adams RP. Identification of Essential Oil Components by Gas Chromatography/Mass Spectroscopy, fourth ed., Allured Publishing Corp; Carol Stream, Illinois, USA 2007.
- [34] Natrajan D, Srinivasan S, Sundar K, Ravindran A. Formulation of essential oil-loaded chitosan-alginate nanocapsules. *J Food Drug Anal.* 2015; 23(3): 560-568. <https://doi.org/10.1016/j.jfda.2015.01.001>
- [35] Borges RS, Keita H, Ortiz BL, dos Santos Sampaio TI, Ferreira IM, Lima ES, de Jesus Amazonas da Silva M, Fernandes CP, de Faria Mota Oliveira AE, da Conceição EC, Rodrigues AB, Filho ACM, Castro AN, Carvalho JC. Anti-inflammatory activity of nanoemulsions of essential oil from *Rosmarinus officinalis* L.: in vitro and in zebrafish studies. *Inflammopharmacology.* 2018; 26(4): 1057-1080. <https://doi.org/10.1007/s10787-017-0438-9>